Journal of Molecular Structure 1125 (2016) 470–480

Contents lists available at ScienceDirect

Journal of Molecular Structure

journal homepage: http://www.elsevier.com/locate/molstruc

Novel aldehyde and thiosemicarbazone derivatives: Synthesis, spectroscopic characterization, structural studies and molecular docking studies

Tuncay Karakurt [a, *], Hakan Tahtaci [b], Nuriye Tuna Subasi [c], Mustafa Er [d], Erbil Ağar [e]

[a] Department of Chemical Engineering, Faculty of Engineering and Architecture, Ahi Evran University, 40100, Kırşehir, Turkey
[b] Department of Polymer Engineering, Faculty of Technology, Karabük University, 78050, Karabük, Turkey
[c] Department of Food Engineering, Faculty of Engineering and Architecture, Ahi Evran University, 40100, Kırşehir, Turkey
[d] Department of Chemical Engineering, Faculty of Engineering, Karabük University, 78050, Karabük, Turkey
[e] Department of Chemistry, Faculty of Arts and Sciences, Ondokuz Mayıs University, 55139, Samsun, Turkey

ARTICLE INFO

Article history:
Received 27 January 2016
Received in revised form
7 July 2016
Accepted 7 July 2016
Available online 11 July 2016

Keywords:
Aldehyde
Thiosemicarbazone
NMR
B3LYP
Beta-lactam

ABSTRACT

In this study our purpose is that, synthesis and characterization of compounds containing the aldehyde and thiosemicarbazone groups and comparison of the theoretical results with the experimental results. The structures of all synthesized compounds were elucidated by IR, ^{1}H NMR, ^{13}C NMR, elemental analyses techniques. The structure of compound (**4**) ($C_9H_8N_4O_2S$) was also elucidated by X-ray diffraction analysis. In addition, the theoretical IR spectrum, ^{1}H NMR and ^{13}C NMR chemical shift values, frontier molecular orbital values (FMO) of these molecules were analyzed by using Becke-3- Lee-Yang-Parr (B3LYP) method with LanL2DZ basis set. Finally, molecular docking studies were performed on synthesized compounds using the 4DKI beta-lactam protein structure to determine the potential binding mode of inhibitors.

1. Introduction

Although recently, there were significant increases in the number of compounds having various biological activities their use has been rather limited because of the emergence of drug resistance to these compounds and their various side effects. For these reasons, chemists have been made a great effort to the development of compounds with biological activity that will be used in pharmaceutical chemistry. Due to having wide-spectrum biological activity of thiosemicarbazone derivatives that synthesis studies made, interest on these compounds has been considerably increased in the pharmaceutical sector at the present time. Supraventricular or ventricular (cardiac arrhythmia) disorders in which the thiosemicarbazone derivative of 3-amino-2-pyridine carboxaldehyde (triapin) [1] that is used as among the rhythm regulators in the treatment is known to be a new third generation antiarrhythmic (rhythm regulators) [2].

Thiosemicarbazones and semicarbazones due to be a small molecule widely used in the treatment of antiviral, anticancer and antiparasital disease. More recently, it has been found that they are highly effective antiparasital compounds against trypanasoma cruzi parasites that cause especially Malaria and Cagas diseases. Generally, thiosemicarbazones show this effect by causing the inhibition of cysteine proteases in this type of parasites and derivatives [3–6]. In higher electroshock applications aryl semicarbazones are known to cause antiepileptic effects on the central nervous system [7–12].

In other study menthone derivatives of thiosemicarbazone and semicarbazones were determined to have anti-HIV activity in an interesting way [13].

In another study of the thiosemicarbazones it was determined that salicyaldehyde thiosemicarbazones act as a pharmacophore (play regulatory role against certain amino acid protein) by forming dicyclic chelates with binding metal ions [14]. A study made on hydroxy derivatives of thiosemicarbazone and semicarbazones lower toxic effects and higher anticancer effects of the hydroxy semicarbazone were drown attention and this type of compounds have been shown to act as a ribonucleotide reductase (RR)

* Corresponding author. Tel.: +90 3862803825.
E-mail address: tuncaykarakurt@gmail.com (T. Karakurt).

http://dx.doi.org/10.1016/j.molstruc.2016.07.013
0022-2860/

inhibitors [15,16].

The biological activity of thiosemicarbazones is due to the aldehyde and ketone functional groups in their structure [17]. It is emphasized with current research in recent years that complex structures of thiosemicarbazone derivatives have antibacterial, antifungal, antiviral and antitumoral [18,19]. Also the copper complex of thiosemicarbazones was determined to have quite high antimicrobial activity especially to a group Streptococcus which cause tonsillitis [20]. It is indicated in studies that acetylacetone thiosemicarbazone and their metal complexes are effective against to *Staphylococcus aureus, Staphylococcus epidermidis* from G(+) bacteria and *Escherichia coli* and *Pseudomonas aeruginosa* from G(−) bacteria [19]. Furthermore, such molecules are reported to be effective against to human cancer cells in the literature [21].

Nowadays, beta-lactam antibiotics are the most commonly used antibiotic derivatives. The most important source of resistance against to beta-lactam antibiotic derivatives of *Enterobacteriaceae* family is beta-lactamase enzymes secreted by the bacteria. Beta-lactamase enzymes are synthesized by mostly gram-negative bacteria, they are believed to be derived from penicillin binding protein due to having similar sequence analyzes and they cause resistance to antibiotics with beta-lactam ring. At the present time there are many identified beta-lactamase enzymes [22]. Beta-lactam antibiotics show their effects by inhibiting the transpeptidase and carboxypeptidases which are responsible for peptidoglycan synthesis and stopping the cell wall [23]. All beta-lactam antibiotics show their effects by binding to target protein which is called penicillin-binding protein (PBP), responsible for the peptidoglycan synthesis in bacterial cell walls on bacterial cytoplasmic membranes. Since peptidoglycan cannot be synthesized, cell wall structure is broken in bacteria whom penicillin binding proteins are inhibited by beta-lactam antibiotics. This situation caused to the loss of osmotic resistance of bacteria and death [24]. *Staphylococcus aureus* is the most important pathogen which synthesizes beta-lactamase in gram-positive bacteria. *Staphylococcus aureus* enzymes are under the control of plasmid and they can pass through the sensitive cells by means of bacteriophages. In case of gram-negative bacteria beta-lactamases are located in the periplasmic space between the outer membrane and cytoplasmic membrane. In gram-negative bacteria, beta-lactamase enzymes are synthesized under the chromosome or plasmid control [25].

In the light of this important data which have been achieved with the literature survey considering that the thiosemicarbazones are biologically active compounds, synthesis of the thiosemicarbazone derivatives expected to show positive activity was carried out (Scheme 1). All of the synthesized compounds are original and their structures were clarified by elemental analysis and spectroscopic methods (FT-IR, NMR). Besides this, the other aim is that; in order to support the experimental studies of the synthesized compound to examine theoretically IR, NMR, UV spectra, potential energy distribution of the vibration frequency (PED) and the frontier molecular orbital (FMO). Additionally, the structures of (**4**) and (**5**) compounds were compared with the ligands of well-known antibacterial targets. Trial docking studies with this enzyme suggested that the crystal structure 4DKI of beta-Lactamase from *S. aureus* as most appropriate target of the (**4**) and (**5**) compounds.

2. Experimental

2.1. Materials and methods

The reactions were carried out under a nitrogen atmosphere using standard Schlenk techniques. The ^{1}H NMR and ^{13}C NMR spectra of the compounds were recorded in DMSO-d_6 using an Agilent NMR VNMRS spectrometer at 400 MHz and 100 MHz, respectively. Chemical shift values are given in ppm (δ) with tetramethylsilane (TMS) as internal standard. The IR spectra were measured in ATR using a Bruker Optics Alpha FT-IR. The mass spectra were measured with a Thermo TSQ Quantum Access Max LC-MS/MS spectrometer equipped with ethyl alcohol and chloroform as solvents. Elemental analyses were performed on a LECO 932 CHNS (Leco-932, St. Joseph, MI, USA) instrument and the results were within ±0.4% of the theoretical values. Melting points were recorded on a Thermo Scientific IA9000 series apparatus and were uncorrected. All of the chemicals were obtained from Sigma Aldrich Chemicals. Theoretical calculations of this study were done by using Gaussian 09 [26] and Gaussview 5.0 [27] package programs. In this study Density Functional Theory (DFT) [28] method is chosen because theoretical calculations of test results which we have done for the analyzed molecules gave the closest value to the experimental results. B3LYP hybrid functional which is one of the most commonly used exchange-correlation functionals that contain Becke's three-parameter exchange function [29–31] and Lee, Yang and Parr's correlation functionals [32] was used in DFT calculation. The LanL2DZ [33–35] base set, which gave the closest value to our experimental results as well and is widely used for large molecules, was selected. Veda4 [36] software was used for PED analysis of the vibration frequency. Molecular docking studies were performed by using Autodock Vina [37] and Discover studio Visualizer 4.5 [38] programs.

2.2. General procedure for the synthesis of 4,4′-((2,3-bis((4-formyl-2,6-dimethoxyphenoxy)methyl)but-2-ene-1,4-diyl)bis(oxy))bis(3,5-dimethoxybenzaldehyde) (**4**)

In a two-necked flask, 4-hydroxybenzaldehyde (**3**) (0.02 mol) and KOH (0.02 mol) were dissolved in absolute ethanol (100 mL) and the solution was stirred for 30 min at room temperature. 1,4-dibromo-2,3-bis(bromomethyl)but-2-ene (**2**) (0.005 mol) was dissolved in absolute ethanol (50 mL) and added drop by drop to this solution at room temperature with the assistance of a dropping funnel. The mixture was then refluxed and stirred for 8–10 h. The progress of the reaction was monitored by TLC at appropriate time intervals. After completion of the reaction, the solution was filtered and the solid matter was obtained. It was washed with deionized water, ethanol and diethyl ether, respectively. The solid matter was recrystallized from DMF-EtOH, 1:2). The synthesized compound was dried with P_2O_5 in a vacuum oven. The physical properties and spectral data of the obtained product are listed below.

This compound was obtained as white crystals, yield 3.26 g (81%), mp 178–179 °C (from DMF-EtOH, 1:2; IR (ATR, cm^{-1}): 3062 (Ar-CH), 2976, 2939 (Aliph. CH), 2839–2737 (CHO), 1684 (C=O), 1583, 1495 (CH=CH), 1117 (−OCH_3), 1322, 1264, 1223 (=C−O−C); ^{1}H NMR (400 MHz, DMSO-d_6, δ ppm): 3.73 (s, 24H, O−CH_3), 4.69 (s, 8H, O−CH_2), Ar−H [7.17 (s, 8H)], 9.85 (s, 4H, CHO); ^{13}C NMR (100 MHz, DMSO-d_6, δ ppm): 56.39 (O−CH_3), 68.61 (O−CH_2), Ar−C [106.87 (CH), 132.27 (C), 141.63 (C), 153.83 (C)], 137.48 (-C=C-), 192.33 (C=O). MS: m/z 826.97 (M + Na, 100). Anal. Calcd. for $C_{42}H_{44}O_{16}$: C, 62.68; H, 5.51. Found: C, 62.59; H, 5.59.

2.3. General procedure for the synthesis of (2E,2′E)-2,2′-((((2,3-bis((4-((E)-(2-carbamothioylhydrazono)methyl)-2,6-dimethoxyphenoxy)methyl)but-2-ene-1,4-diyl)bis (oxy))bis(3,5-dimethoxy-4,1-phenylene))bis(methanylylidene))bis(hydrazine carbothioamide) (**5**)

Compound (**5**) was synthesized according to a method given in the literature [39]. In a round-bottomed flask, compound (**4**) (0.0025 mol) and thiosemicarbazide (0.015 mol) were heated to

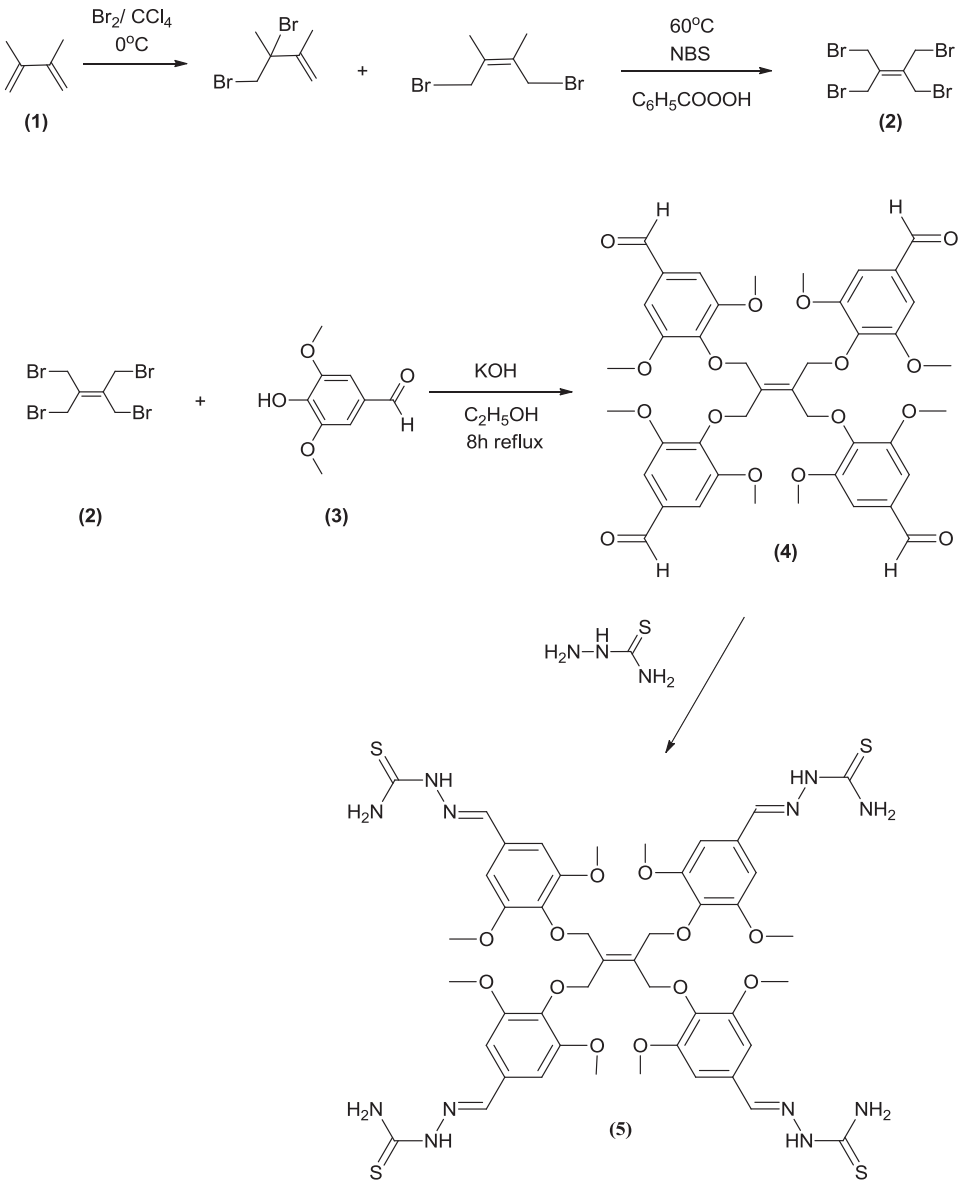

Scheme 1. Synthetic route for the synthesis of the target compounds.

140 °C without solvent in an oil bath and stirred for 1 h. After the completion of the reaction, DMF (20 mL) was added to the reaction content and dissolved. Water was then added to the solution and a solid precipitated. The solution was filtered and the solid was obtained. The solid was washed with warm water and absolute ethanol to remove excess thiosemicarbazide and impurities. The solid was recrystallized from DMF/ethanol (1:1). The synthesized compound was dried with P_2O_5 in a vacuum oven. The physical properties and spectral data of the obtained product are listed below.

This compound was obtained as gray solid, yield 2.08 g (76%), mp 230 °C (decomp.) (from DMF-EtOH, 1:1); IR (ATR, cm^{-1}): 3259–3156 (NH_2), 3162 (–NH–), 3042 (Ar-CH), 2944 (Aliph. CH), 1577 (CH=CH), 1518 (C=N), 1323, 1273, 1233 (=C–O–C), 1123 ($-OCH_3$); ^1H NMR (400 MHz, DMSO-d_6, δ ppm): 3.71 (s, 24H, O–CH_3), 4.58 (s, 8H, O–CH_2), Ar–H [7.04 (s, 8H)], 7.93 (s, 4H, CH=N), 8.07 (s, 4H, NH_2), 8.19 (s, 4H, NH_2), 11.40 (s, 4H, –NH); ^{13}C NMR (100 MHz, DMSO-d_6, δ ppm): 56.45 (O–CH_3), 68.82 (O–CH_2), Ar–C [104.85 (CH), 130.20 (C), 138.07 (C), 153.82 (C)], 137.53 (-C=C-), 142.69 (CH=N), 178.17 (C=S).

MS: m/z 1098.19 (M^+, 100). Anal. Calcd. for $C_{46}H_{56}N_{12}O_{12}S_4$: C, 50.35; H, 5.14; N, 15.32 Found: C, 50.44; H, 5.28; N, 15.25.

3. Crystal structure determination

X-ray diffraction data of crystal was collected with a Bruker AXS APEX CCD [40] diffractometer by using MoKα beam. Structure solving of the crystal was obtained by using direct methods with the SHELXT-2014 [41] program. In solving process, refinement process was carried out with SHELXL-2014 [42] program which uses full matrix the least squares method to determine the positions of atoms other than hydrogen. Isotropic refinement was performed in order to become more sensitive position of atoms in the first stage of the treatment and for the determination of missing atoms. As a result of refinement process, the absence of missing atoms other than hydrogen was observed and an anisotropic refinement was performed. Hydrogen atoms were determined at the next stage of refinement. Hydrogen atom positions were obtained geometrically according to the overlap method. When placing hydrogen atoms geometrically an aromatic C–H bond

length was fixed at 0.93 Å, methylene (-CH_2) bond length at 0.97 Å and methyl (-CH_3) bond length at 0.96 Å. After the process of structure solving and refinement, ORTEP-3 [43] program was used for molecular drawings, WinGX [44] and MERCURY [45] programs were used for the calculations.

4. Results and discussion

Compound (**2**) was synthesized according to a method given in the literature [39]. In the first part of the study, 4,4′-((2,3-bis((4-formyl-2,6-dimethoxyphenoxy)methyl)but-2-ene-1,4-diyl) bis(oxy))bis(3,5-dimethoxybenzaldehyde) (**4**) was obtained in good yield (81%) from the reaction of 4-hydroxy-3,5-dimethoxy benzaldehyde (**3**) with 1,4-dibromo-2,3-bis(bromomethyl)but-2-ene (**2**) in the presence of KOH and absolute alcohol (Scheme 1). In the second part of the study, thiosemicarbazone derivative (**5**) having the role of target compound was synthesized in high yield (76%) by a condensation reaction of (4,4′-((2,3-bis((4-formyl-2,6-dimethoxyphenoxy)methyl)but-2-ene-1,4-diyl)bis(oxy))bis(3,5-dimethoxy benzaldehyde) (**4**) with thiosemicarbazide (Scheme 1).

4.1. X-ray structure analysis of crystal (*4*)

The structure of compound (**4**) ($C_{42}H_{44}O_{16}$) was supported by X-ray diffraction analysis. The structural parameters of the crystal and the details of data collection and refinement process are given in Table 1. Molecule's ORTEP diagram drawing with experimental 40% probability ellipsoids and input molecule used in Gaussian 09 program are given Fig. 1 a The optimized structures of the molecules (**4**) and (**5**) that obtained from theoretical calculations are shown in Fig. 1b–c.

The compound (**4**) has non-planar dimethoxybenzaldehyde rings (A(C1–C6) ring and B(C14–C19) ring). Dihedral angle between A and B rings is 79.15° (**9**). In similar molecule this angle was observed as 76.43° (**8**) in the literature [46]. The molecular structure of (**4**) is shown in Fig. 1 a The asymmetric unit contains half a molecule and the complete molecule is generated by a crystallographic 2-fold axis with direction at 1/2-x,y,-z. The molecule exists in a Z configuration with respect to the two carbon C11 = C12 bonds [1.329 (3) Å]. This bond length was found to be shorter than C–C bond length of the molecule. In the literature this length was observed as 1.332(6) Å [47], 1.335(5) Å [47] and 1.318(6) Å) [48]. Likewise, while bond lengths of C11–C10, C12–C13, C10–O4 and C13–O5 were observed as 1.506(3), 1.505(3), 1.445(2) and 1.445(2) Å, respectively. In the literature these bond lengths were given as 1.504(3), 1.502(3), 1.434(3) and 1.451(3) Å [49].

The experimental and the calculated bond length and bond angles of the crystal (**4**) are shown in Table 2.

Intermolecular C–H···O and intramolecular C–H···O hydrogen bonds were observed in the crystal. The molecules are bonded to each other with these interactions. It was observed that intermolecular C–H···O hydrogen bonds of crystal (**4**) formed the $R_2^2(30)$ closed ring according to the symmetry center. C20 atoms in the bond formed for the crystal acts as a hydrogen bond donors to O2 atom which is at 1−x,1−y,−z position by means of H20 atom (Fig. 2). C10–H10···O3 intramolecular hydrogen bond was observed to form the S(6) closed ring. The data related to the hydrogen bonds are given in Table 3.

Symmetry operation operators that allow the crystal to repeat itself in the 3-dimensional space are shown in Fig. 3 (yellow circle = inversion, purple line = sliding plane, green line = 2-axis rotation, brown line = 2-screw axis of symmetry processor).

4.2. IR studies

Molecule (**4**) containing 24 atoms has C1 symmetry point group and 300 fundamental vibration frequency while the molecule (**5**) has C1 symmetry point group and 384 fundamental vibration

Table 1
Data collection and refinement values of compound (**4**).

Chemical formula	$C_{42}H_{44}O_{16}$
Formula weight	804.77 (a.k.b)
Temperature	293 K
Wavelength	MoK_α, 0,71073 Å
Crystal system	Monoclinic
Space group	I2/a
Diffractometer/measurementmethod	Bruker AXS APEX CCD/ω-scan
Unit cell parameters	
a	14.740(12)Å
b	16.500(14)Å
c	16.591(14)Å
α	90°
β	102.369(6)°
γ	90°
Volume	3940.5(6) $Å^3$
Z	4
Calculated density	1.357 gr cm^{-3}
μ	0.105 mm^{-1}
F(000)	1696
crystal size (mm)	0.44 × 0.22 × 0.16
Theta range for data collection collection	2.99°–28.35°
Index ranges	$-19 \le h \le 18$, $-22 \le k \le 21$, $-22 \le l \le 22$
Measured reflections	47846
Independent/	4910
Observed reflections [$I>2\sigma(I)$]	3352
Absorption correction	Integration (X-RED32)
Weighting scheme	$w = 1/[\sigma^2(F_0^2)+(0.0692P)^2 + 4.0624P]$ $P=(F_0^2 + 2F_c^2)/3$
R_{int}	0.0539
Refinement method	Full-matrix least-squares on F^2
Goodness–of–fit on indicator(S)	1.045
R, wR	0.0566, 0.1349
Extinction coefficient	0.004(8)
$(\Delta\sigma)_{max}$, $(\Delta\sigma_{min})$ (e/$Å^3$)	0.67, −0.22

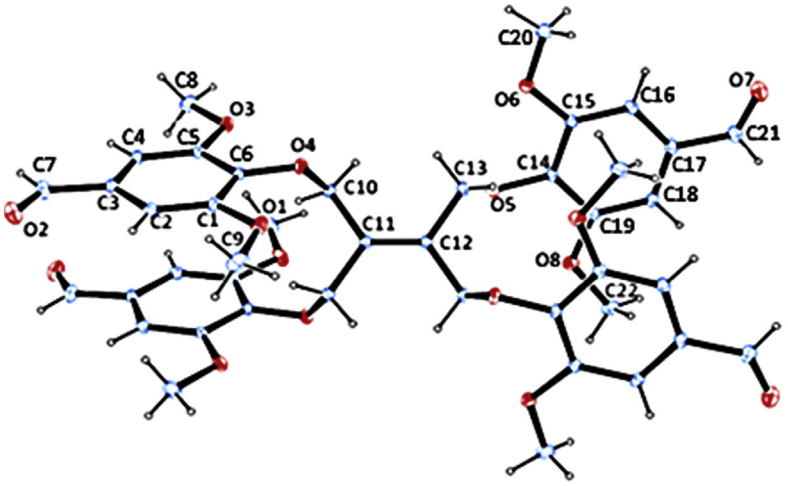

(a)

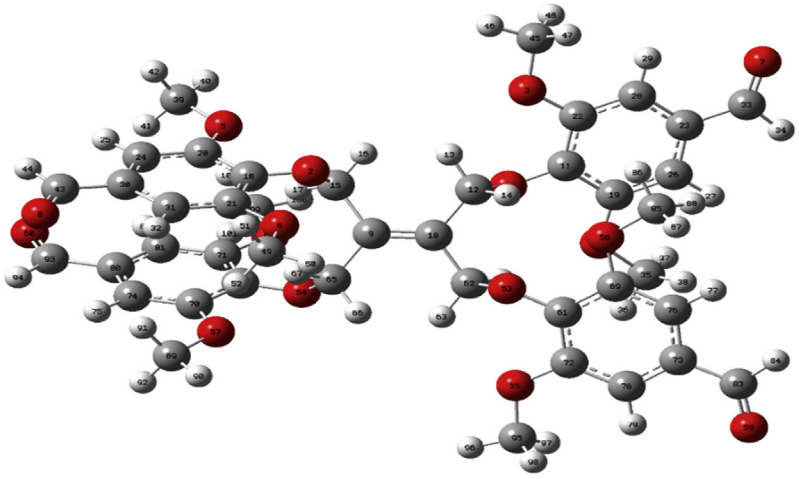

(b)

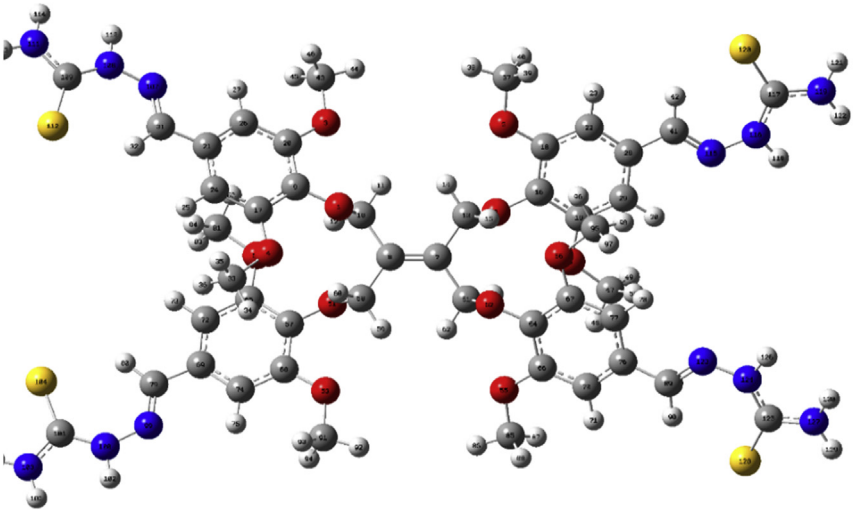

(c)

Fig. 1. (a) ORTEP-3 shape of $C_{42}H_{44}O_{16}$ (**4**) crystal (b) Calculated shape (**4**) crystal (c) Calculated shape of (**5**) crystal.

Table 2
Experimental and theoretical parameters belonging to compound (**4**).

Bond length(Å)	Exp.	Cal.(DFT)
O5–C14	1.370(2)	1.383
O5–C13	1.445(2)	1.498
O4–C10	1.445(2)	1.498
O4–C8	1.365(2)	1.382
O6–C15	1.364(3)	1.386
O6–C16	1.427(3)	1.458
O8–C21	1.359(3)	1.395
O8–C22	1.425(3)	1.459
O3–C6	1.362(2)	1.394
O3–C7	1.426(3)	1.459
O1–C1	1.367(3)	1.392
O1–C9	1.421(3)	1.458
O7–C19	1.176(3)	1.253
O2–C4	1.195(3)	1.252
C11–C12	1.329(3)	1.361
C11–C10	1.506(3)	1.511
C12–C13	1.505(3)	1.513
C14–C21	1.394(3)	1.420
C14–C15	1.406(3)	1.426
C8–C6	1.397(3)	1.422
C8–C1	1.398(3)	1.420
C6–C5	1.384(3)	1.402
C1–C2	1.385(3)	1.407
C15–C17	1.387(3)	1.402
C18–C20	1.382(3)	1.409
C18–C19	1.479(3)	1.476
Bond Angles(°)		
C14–O5–C13	115.5(1)	120.4
C10–O4–C8	116.5(1)	119.1
C15–O6–C16	117.4(2)	118.4
C21–O8–C22	117.9(2)	118.5
C6–O3–C7	117.5(2)	118.4
C1–O1–C9	117.5(2)	118.4
C12–C11–C10	123	123.6
C11–C12–C13	123.3(2)	123.1
O5–C14–C21	118.2(2)	117.8
O5–C14–C15	121.6(2)	122.9
O1–C1–C2	125.0(2)	124.4
C5–C3–C2	121.5(2)	120.8
C2–C3–C4	120.3(2)	119
C1–C2–C3	118.9(2)	119.7

Table 3
Hydrogen bond geometry for compound (**4**) $C_{23}H_{25}N_3OS$ single crystal (Å, °).

D-H···A	D-H	H···A	D···A	D-H···A
C20– H20···O2^{i}	0.86 (3)	2.28(3)	3.11(2)	162(3)
C10– H10···O3	0.82(2)	1.93(2)	2.65(3)	146(2)

Symmetry codes: i = 1−x, 1−y, −z.

frequency. In this study, all calculations of the vibration frequency, supported by potential energy distribution (PED) analysis, were done by using DFT(B3LYP/LanL2DZ) basis set. Experimental and calculated spectra are shown in Figs. 4–5. To match the calculation results with the experimental results for each frequency value is multiplied by the scale value 0.961 [50].

Analyzing the IR spectral data of these compounds the most significant spectral data for compound (**4**) is CHO (fermidublet) absorption band of an aldehyde which is observed at between the ranges of 2839–2737 cm^{-1}. In the literature experimentally this band was observed as 2724-2894 cm^{-1} [51], 2796–2894 [47] and 2875-2756 cm^{-1}, respectively [52]. This vibration was calculated theoretically in the range of 2856–2850 cm^{-1} with 100–98% PED contribution which consist of pure C–H modes. Accordingly, because the molecule is symmetrical C=O absorption bands that bearing an important and specific bands in such compounds was observed experimentally at 1684 cm^{-1}. In the literature this band was observed at 1672 [51], 1671–1656 [52] and 1698 cm^{-1} [47]. Theoretically it was calculated at between the range of 1603–1600 cm^{-1} with 67–58% PED contribution which consist of pure C=O modes.:–CH absorption band for the aromatic ring in the compound was observed at 3062 cm^{-1}, C–O–C bands at 1322, 1264 and 1223 cm^{-1}; it has been found that observation of these values supported the proposed structure. These vibration modes were calculated between the range of 3114–3094 and 1298–1294 cm^{-1}.

When IR spectral data of compound (**5**) analyzed, it was determined that C=O absorption band of the aldehyde functional group used in the synthesis of these compounds was completely disappeared and instead of this the band of azomethine group (C=N) was appeared at frequency of 1577 cm^{-1}. This calculated value is given as 1601 cm^{-1} in the literature [53]. This vibration was calculated at between the range of 1605–1592 cm^{-1} with 14–11% PED contribution that consist of pure C=N modes.

Another important data that proved the formation of thiosemicarbazone derivatives (**5**) is that observation of $-NH_2$ symmetric and asymmetric absorption bands at between the range of 3259–3156 cm^{-1} and –NH absorption band at 3162 cm^{-1}. Observed symmetric and asymmetric vibration frequencies of $-NH_2$ group are given at 3330–3450 and 3150–3270 cm^{-1} [54], and the –NH vibration frequency is given as 3262 cm^{-1} in the literature [55]. These vibration modes have been calculated as in the range 3602–3600 cm^{-1} with 97% PED contribution that consist of pure $-NH_2$ modes and as between the range of 3476–3475 cm^{-1} with 88% PED contribution that consist of pure –NH modes, respectively.

4.3. NMR studies

GIAO (Gauge-Independent Atomic Orbital) [56,57] method was

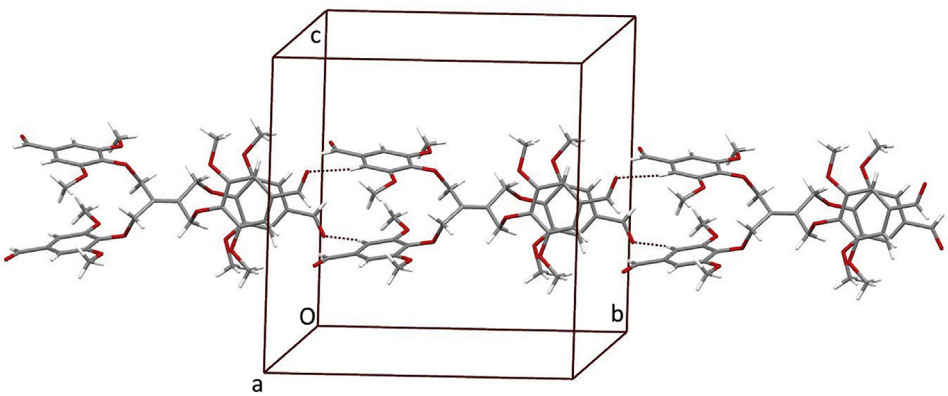

Fig. 2. Representation of intermolecular C–H···O interactions of (**4**) crystal along the a axis.

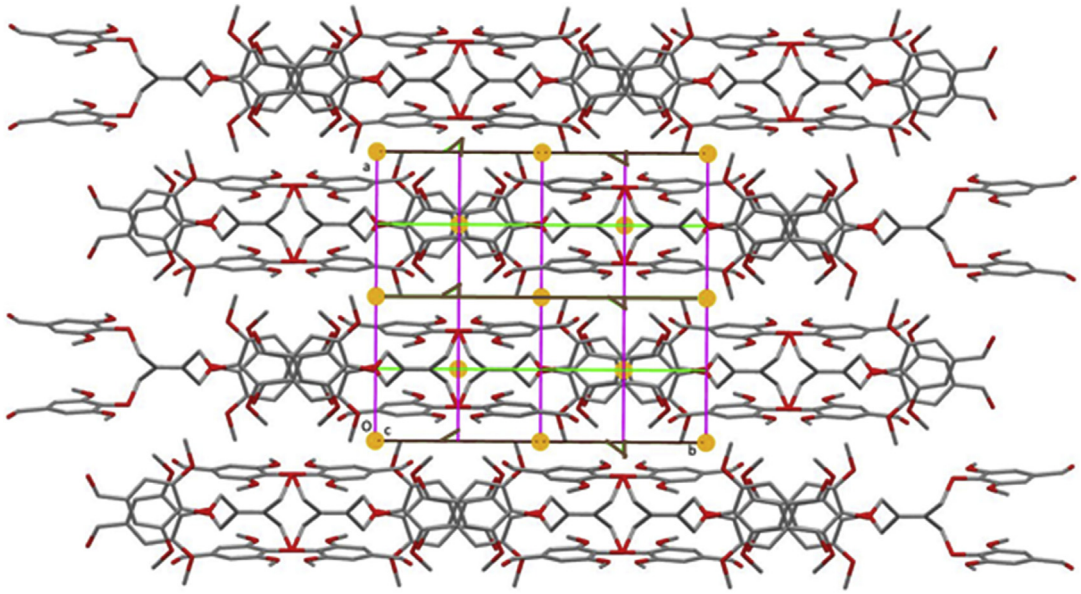

Fig. 3. Crystal (**4**) packed with symmetry operation operators.

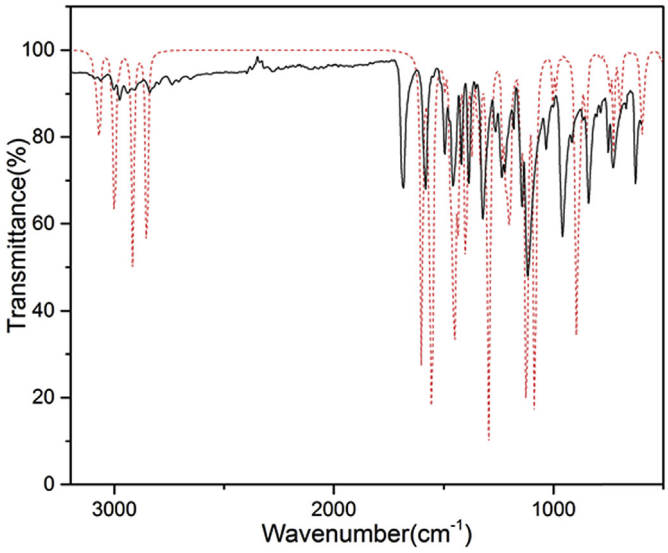

Fig. 4. Comparison Experimental (straight-line) and theoretical (dashed line) FT-IR spectra for the molecule (**4**).

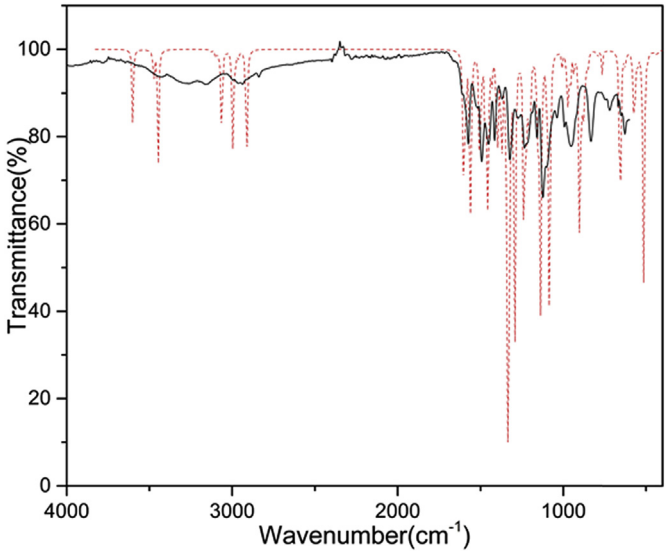

Fig. 5. Comparison Experimental (straight-line) and theoretical (dashed line) FT-IR spectra for the molecule (**5**).

used to determine the NMR chemical shifts of molecule (**4**) and (**5**) and TMS (tetramethylsilane) was used as a reference calculated ^{1}H NMR and ^{13}C NMR chemical shift values selected dimethyl sulfoxide (DMSO) for TMS are 32.1 and 184.2 ppm for DFT/B3LYP/Lan2LDZ, respectively. Experimental and calculated NMR spectra are shown in the Supplementary Material, Figs. S1 and S2.

The structure of the compound (**4**) was confirmed with the assistance of ^{1}H NMR spectroscopy. When analyzed the ^{1}H NMR spectra of this compound, aldehyde group (CHO) proton was observed at 9.85 ppm as a singlet that is corresponding to 4 protons. This chemical shift value is specific for the aldehyde protons. This value is given as 10.05–10.18 and 10.83–9.86 ppm in the literature. Calculated chemical shift value of this peak was obtained as 10.03 ppm. Proton signals which belong to the $-OCH_2$ and $-OCH_3$ of this compound are recorded as a singlet at 4.69 ppm corresponds to 8 protons and at 3.73 ppm corresponds 24 protons, respectively. In the literature, proton signal of $-OCH_2$ was observed as 4.23–4.53 [51] and 4.98–4.73 [52] ppm and proton signal of $-OCH_3$ was observed as 3.70 [51] and 3.83 ppm [52]. Theoretically these two peaks were calculated between the range of 5.82–5.20 and 2.44–3.75 ppm. In compound ^{13}C NMR spectrum, while $-OCH_2$ carbon peak signal was recorded at 68.61 ppm as expected from sp^3 hybridized carbon atoms, $-OCH_3$ carbon bonded to the aromatic ring was appeared at 56.53 ppm. In the literature, these two shift values were observed at 56–65 [46] and 55.55 ppm [52], respectively. Theoretically, these peaks are calculated at 73.10–71.95 and at 55.06–54.94 ppm. On the other hand, sp^2 hybridized C=C and C=O carbon signals were recorded as expected at 137.48 ppm and at 192.33 ppm, respectively. These two values are calculated in the range of 138.87–136.77 and 199.36–199.49 ppm.

The structure of the compound (**5**) which is a thiosemicarbazone derivative was confirmed by ^{1}H NMR spectrum. In

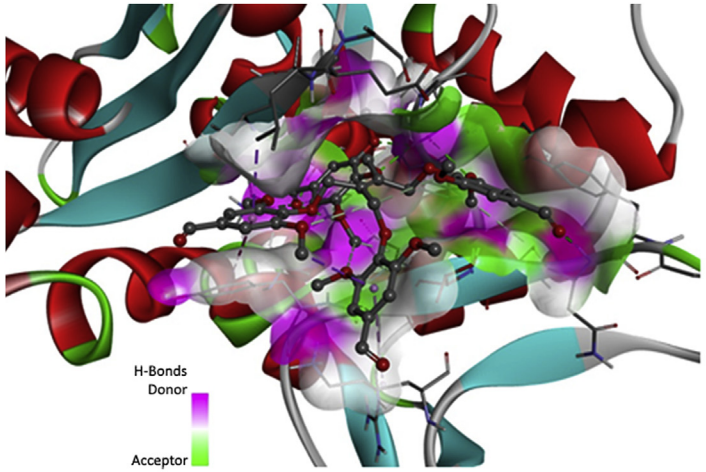

(a)

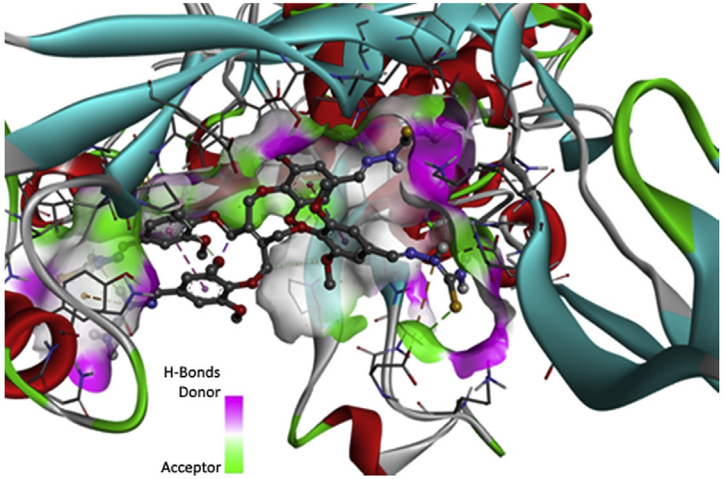

(c)

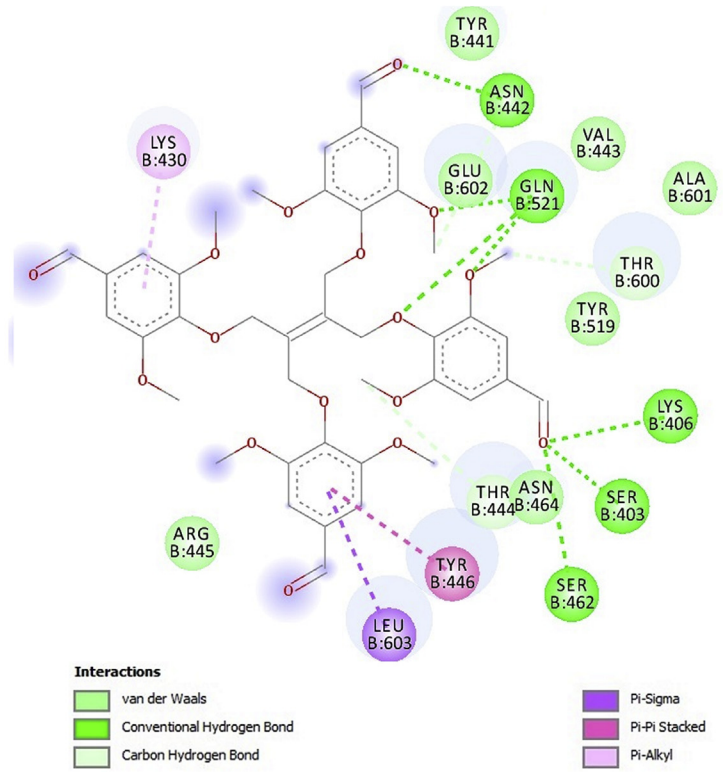

(b)

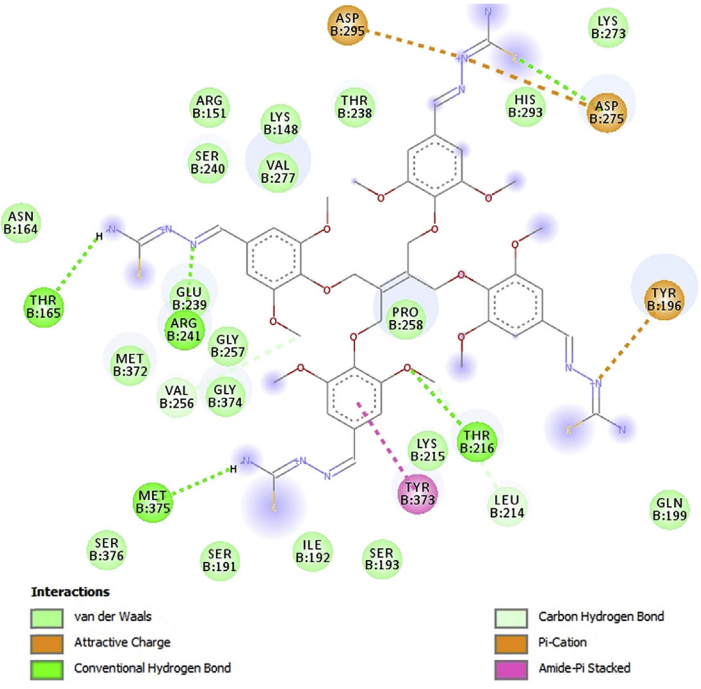

(d)

Fig. 6. Docking result representation of (a), (b) (**4**) compound; (c), (d) (**5**) compound. H-bonding, π-π and π-alkyl interactions are shown with green, pink and orange lines, respectively. (For interpretation of the references to colour in this figure legend, the reader is referred to the web version of this article.)

^{1}H NMR spectrum of this compound it was observed that aldehyde proton of (**4**) (CHO) occurring at about 9.85 ppm are replaced by the proton peak of azomethine group (CH═N) which is appeared at 7.93 ppm. This value was calculated theoretically as between the range of 9.86–9.85 ppm. On the other hand, while −NH proton gains relatively acidic nature in this compound and it was appeared at about 11.40 ppm as a singlet, the protons bonded to nitrogen atom (NH_2) were observed at 8.07 and 8.19 ppm as a singlet in spectral data although at first they seem to be equivalent protons. In the D_2O-exchangeable spectra of compound (**5**), disappeared the singlet belonging to −NH proton in the 11.40 ppm and NH_2 protons appeared at 8.07 and 8.19 ppm supported our suggested structures. Observed CH═N and NH_2 group protons are given in the literature at 10.06 and 8.57–7.56 ppm, respectively [58]. The peaks of −NH and NH_2 protons were calculated in the range of 7.72–7.59 and 4.70–4.62 ppm.

Chemical shifts of −NH and NH_2 peaks were obtained as almost half of the experimental results in the theoretical calculations. In this case, it is drown a conclusion that there is a possible intermolecular hydrogen bond N–H···N in the molecule and free calculation were done theoretically assuming that there is no hydrogen bond.

When analyze the ^{13}C NMR spectrum of the compound, C═C, $-OCH_2$ carbon atoms of the molecule and aromatic carbon atoms were found to show great similarity with the spectral data which is given in the molecule (**4**). However, in the molecule (**5**) the most significant and different spectral data that belongs to the (C═S) group is appeared at about 178.17 ppm. This spectral data is quite specific value in the thiosemicarbazone derivatives, thiourea and thioamides [59–62]. It is theoretically calculated as in the range of 186.3–185.80 ppm. On the other hand, carbon signals of azomethine (C═N) group were recorded at 142.69 ppm and they were calculated theoretically between the range of 147.27–148.87 ppm. Other spectral data belonging to the carbon skeleton of the molecule completely confirms our proposed molecular structure.

4.4. Frontier molecular orbital analysis

After obtaining stable structure and structural parameters of the molecule (**4**) and (**5**), HOMO and LUMO energy values were analyzed and the hardness parameters were obtained from these energies. How this property is changed with the effect of the different groups were investigated.

The most important orbitals in a molecule are frontier molecular orbitals which are called HOMO and LUMO. The energy difference between these two orbitals is a measure of the chemical stability of the molecule and since it is a measurement of the electron conductivity, it is a critical parameter determining the molecular electrical transport properties. Therefore, this energy difference is largely responsible for the chemical and spectroscopic properties of molecules [63].

The HOMO and LUMO of a molecule are significant for intermolecular interactions [64], between the HOMO of the drug with the LUMO of the receptor and vice versa. Energy gap between the interacting orbitals determines the stabilization of the intermolecular interactions. Increasing HOMO energy and decreasing LUMO energy in the drug and receptor molecule causes the more stabilizing interactions [65].

Calculations have been carried out in the gas phase, when the HOMO energy values were calculated as −6.00 for the molecule (**4**) and −5.32 eV for the molecule (**5**). The LUMO energy values were calculated as −2.12 eV for the molecule (**4**) and as −1.55 eV for the molecule (**5**). The difference between this energy levels ($\Delta E_{HOMO-LUMO}$) was calculated as 3.88 eV for the molecule (**4**), 3.77 eV for the molecule (**5**).

Nevertheless, the compound (**5**) has more stable interaction member with lowest energy gap (3.77 eV) from compound (**4**), which may be explained the higher binding interaction with binding site of Beta-lactam crystal structure.

The distributions and energy levels of the HOMO and LUMO orbitals and corresponding density of state (DOS) of (**4**) and (**5**) structures are shown in the Supplementary Material, Fig. S3.

Molecular hardness parameters were obtained from finite difference formula proposed by Paar and Pearson [66,67], and they were calculated by using the operational definition of η:

$$\eta = 1/2\ (IE - EA)$$

In this formula, IE shows the first ionization energy and EA shows the electron affinity. Hardness value can provide the following approach by means of the highest occupied molecular orbital energy (E_{HOMO}) and the lowest unoccupied molecular orbital energy (E_{LUMO}):

$$\eta \approx 1/2(E_{LUMO} - E_{HOMO})$$

Some studies in the literature, the effect of hardness parameters on the charge transfer are examined and in these studies it is indicated that small value of η corresponds to a more powerful charge transfer interaction [68–70]. Calculated hardness values for the molecule (**4**) and (**5**) are 3.88 and 3.77, respectively. Observing the calculated hardness value of molecule (**5**) is smaller than the molecule (**4**) shows that charge transfer would be stronger in the molecule.

4.5. Molecular docking studies

Beta-lactam crystal structure (pdb code: 4DKI) for the docking studies was provided via Protein Data Bank (http://www.rcsb.org/pdb). Before the docking operation the water molecules were

Table 4
Affinity and RMSD values different conformations of compound (**4**) and (**5**). The minimum RMSD values are shown in bold.

Compound (**4**)			Compound (**5**)		
Mode	Affinity (kcal/mol)	Distance from best mode RMSD	Mode	Affinity (kcal/mol)	Distance from best mode RMSD
1	−6.3	0.000	1	−6.4	0.000
2	−6.3	49.217	2	**−6.3**	**1.261**
3	−6.2	1.067	3	−6.3	4.017
4	−6.2	1.603	4	−6.2	2.902
5	**−6.2**	**0.625**	5	−6.2	3.692
6	−6,1	1.666	6	−6.1	7.677
7	−6.1	49.162	7	−6.1	5.056
8	−6.0	49.230	8	−6.1	4.054
9	−6.0	47.242	9	−6.0	4.170

removed from the structure 4DKI, hydrogen atoms and Gasteiger charges were added. After these processes, docking was made to the target molecule binding site of ligand (**4**) (Fig. 6(a)) and (**5**) (Fig. 6(c)). Autodock Vina was used for docking studies and AutoDock Tools was used to create Docking input files. Receptor ligand interactions are indicated by the Discover Studio Visualizer 4.5 software. The prediction of binding energy (docking score) and RMSD values are obtained after molecular docking and computational results are shown comparatively in Table 4.

The obtained docking results are stated as correct when the RMS value is smaller than 2 Å [71]. RMSD value is the root mean square deviation from the determined structural conformation of the ligand. In other words, it means that the deviation from the active site of the ligand to interact and it is the most important criteria for the docking results. The binding energy is the criteria that looked after the RMSD values. The reason of this priority is that the molecule may also give lower binding energy with a place other than the active region. Therefore, first looking at its proximity to the active site, and then looking at its binding energy which is made in the active region. Docking results for the molecule **4**, binding energy that is corresponded to the lowest RMSD value is −6.2 kcal/mol and −6.3 kcal/mol for the molecule **5**.

It was observed that ligands bonded to the substrate binding site of receptors with a weak non-covalent interaction and they were bonded more specifically with hydrogen bonding, van der Waals, π-π and π-alkyl interactions. As shown in Fig. 6(b, d) hydrogen bonds were formed between SER403, LYS406, ASN442, SER462, GLN521 and O atoms for ligand (**4**) at 1.96, 2.77/2.82, 2.27, 2.88 and 2.48/2.20/2.67 Å in length and for ligand (**5**) between THR216, ARG241, TYHR165, MET375 and ASP275 with O and N atoms at 2.65, 2.31, 2.61, 2.63 and 3.48 Å in length, respectively. Furthermore, as shown in Fig. 6 (b, d) while LEU603 was attached to the ligand (**4**) with π-sigma interaction, TYR446 with π-π interaction and LYSB430 with π-alkyl interaction; TYR196, TYR373 and GLY374 were attached to the ligand (**5**) with π-cation and amide-π interactions, respectively. According to the calculated binding affinity ligand (**4**) and (**5**) have been identified as inhibitor candidate molecules for beta-lactam target structure. Consequently, these potential inhibitor compounds which are found will be hoping for us to design drugs with high selectivity and have low side effects in new studies that will be done in the future.

5. Conclusions

In this study, aldehydes and compounds containing thiosemicarbazone group were synthesized easily with the applicable methods in high yield. The structures of all synthesized compounds were clarified by various spectroscopic methods.

Among the synthesized compounds (**4**) and (**5**), single-crystal versions of compound (**4**) was obtained. After the stable structures and structural parameters of these compounds were calculated, their IR, NMR spectra, HOMO and LUMO energies and hardness parameters of these energies were found.

The effect of aldehyde and thiosemicarbazone groups in the (**4**) and (**5**) on these properties was investigated. Obtaining the smaller hardness value of (**5**) than molecule (**4**) shows that there is a strong charge transfer in this molecule. At the same time, docking simulation process was applied to obtain possible bonding patterns and conformation for ligands (**4**) and (**5**). According to the calculated bonding affinities, all compounds in this study were determined to be inhibitor candidates for the beta-lactamase target structure.

Acknowledgement

This study was supported financially by the Research Centre of Ahi Evran University (PYO-MYO.4001.14.002).

Appendix A. Supplementary data

Supplementary data related to this article can be found at http://dx.doi.org/10.1016/j.molstruc.2016.07.013.

References

[1] Winder, P. Collins, D. Whelan, Effects of ethionamide and isoxyl on mycolic acid synthesis in Mycobacterium tuberculosis BCG, Microbiol. 66 (3) (1971) 379–380.
[2] M. Spaniol, R. Bracher, H.R. Ha, F. Follath, S. Krähenbühl, Toxicity of amiodarone and amiodarone analogues on isolated rat liver mitochondria, J. Hepatol. 35 (5) (2001) 628–636.
[3] D.C. Greenbaum, Z. Mackey, E. Hansell, P. Doyle, J. Gut, C.R. Caffrey, J. Lehrman, P.J. Rosenthal, J.H. McKerrow, K. Chibale, Synthesis and structure-activity relationships of parasiticidal thiosemicarbazone cysteine protease inhibitors against Plasmodium falciparum, Trypanosoma brucei, and Trypanosoma cruzi, J. Med. Chem. 47 (12) (2004) 3212–3219.
[4] R.A. Finch, M.-C. Liu, A.H. Cory, J.G. Cory, A.C. Sartorelli, Triapine (3-aminopyridine-2-carboxaldehyde thiosemicarbazone; 3-AP): an inhibitor of ribonucleotide reductase with antineoplastic activity, Adv. Enzyme Regul. 39 (1) (1999) 3–12.
[5] H.R. Wilson, G.R. Revankar, R.L. Tolman, In vitro and in vivo activity of certain thiosemicarbazones against Trypanosoma cruzi, J. Med. Chem. 17 (7) (1974) 760–761.
[6] X. Du, C. Guo, E. Hansell, P.S. Doyle, C.R. Caffrey, T.P. Holler, J.H. McKerrow, F.E. Cohen, Synthesis and structure-activity relationship study of potent trypanocidal thio semicarbazone inhibitors of the trypanosomal cysteine protease cruzain, J. Med. Chem. 45 (13) (2002) 2695–2707.
[7] P. Yogeeswari, D. Sriram, S. Mehta, D. Nigam, M.M. Kumar, S. Murugesan, J. Stables, Anticonvulsant and neurotoxicity evaluation of some 6-substituted benzothiazolyl-2-thiosemicarbazones, Il Farm. 60 (1) (2005) 1–5.
[8] J.P. Leach, Polypharmacy with anticonvulsants, CNS Drugs 8 (5) (1997) 366–375.
[9] S.a.J. Czuczwar, K. Przesmycki, Felbamate, gabapentin and topiramate as adjuvant antiepileptic drugs in experimental models of epilepsy, Pol. J. Pharmacol. 53 (1) (2001) 65–68.
[10] S.J. Hays, M.J. Rice, D.F. Ortwine, G. Johnson, R.D. Schwarz, D.K. Boyd, L.F. Copeland, M.G. Vartanian, P.A. Boxer, Substituted 2-benzothiazolamines as sodium flux inhibitors: quantitative structure–activity relationships and anticonvulsant activity, J. Pharm. Sci. 83 (10) (1994) 1425–1432.
[11] J. Mizoule, B. Meldrum, M. Mazadier, M. Croucher, C. Ollat, A. Uzan, J.-J. Legrand, C. Gueremy, G. Le Fur, 2-Amino-6-trifluoromethoxy benzothiazole, a possible antagonist of excitatory amino acid neurotransmission–I: anticonvulsant properties, Neuropharmacology 24 (8) (1985) 767–773.
[12] R.S. Chopade, R.H. Bahekar, P.B. Khedekar, K.P. Bhusari, R. Rao, A. Raghu, Synthesis and anticonvulsant activity of 3-(6-Substituted-benzothiazol-2-yl)-6-phenyl-[1, 3]-xazinane-2-thiones, Arch. Pharm. 335 (8) (2002) 381–388.
[13] V. Mishra, S. Pandeya, C. Pannecouque, M. Witvrouw, E. De Clercq, Anti-HIV activity of thiosemicarbazone and semicarbazone derivatives of (±)-3-Menthone, Arch. Pharm. 335 (5) (2002) 183–186.
[14] K.J. Duffy, A.N. Shaw, E. Delorme, S.B. Dillon, C. Erickson-Miller, L. Giampa, Y. Huang, R.M. Keenan, P. Lamb, N. Liu, Identification of a pharmacophore for thrombopoietic activity of small, non-peptidyl molecules. 1. Discovery and optimization of salicylaldehyde thiosemicarbazone thrombopoietin mimics, J. Med. Chem. 45 (17) (2002) 3573–3575.
[15] S. Ren, R. Wang, K. Komatsu, P. Bonaz-Krause, Y. Zyrianov, C.E. McKenna, C. Csipke, Z.A. Tokes, E.J. Lien, Synthesis, biological evaluation, and quantitative structure-activity relationship analysis of new Schiff bases of hydroxysemicarbazide as potential antitumor agents, J. Med. Chem. 45 (2) (2002) 410–419.
[16] J. Patole, S. Padhye, M. Moodbidri, N. Shirsat, Antiproliferative activities of iron and platinum conjugates of salicylaldehyde semi-/thiosemicarbazones against C6 glioma cells, Eur. J. Med. Chem. 40 (10) (2005) 1052–1055.
[17] K. Hu, Z.-h. Yang, S.-S. Pan, H.-j. Xu, J. Ren, Synthesis and antitumor activity of liquiritigenin thiosemicarbazone derivatives, Eur. J. Med. Chem. 45 (8) (2010) 3453–3458.
[18] F. Islam, A.S.M. Mohsin, J.A. Khanam, Hepatoprotective effect of acetone semicarbazone on Ehrlich ascites carcinoma induced carcinogenesis in experimental mice, Asian. Pac. J. Trop. Biomed 3 (2013) 105–110.
[19] J.G. Da Silva, C.C. Perdigao, N.L. Speziali, H. Beraldo, Chalcone-derived thiosemicarbazones and their zinc (II) and gallium (III) complexes: spectral studies and antimicrobial activity, J. Coord. Chem. 66 (3) (2013) 385–401.
[20] E. Pahontu, V. Fala, A. Gulea, D. Poirier, V. Tapcov, T. Rosu, Synthesis and characterization of some new Cu (II), Ni (II) and Zn (II) complexes with salicylidene thiosemicarbazones: antibacterial, antifungal and *in vitro* antileukemia activity, Molecules 18 (8) (2013) 8812–8836.
[21] G. Ermut, N. Karali, İ. Çetin, M. Topçu, S. Birteksöz, Synthesis and chemotherapeutic activities of 5-Chloro-1h-Indole-2,3-Dione 3-Thiosemicarbazones, Mar. Pharm. J. 17 (2013) 147–154.

[22] P.A. Bradford, Extended-spectrum β-lactamases in the 21st century: characterization, epidemiology, and detection of this important resistance threat, Clin. Microbiol. Rev. 14 (4) (2001) 933–951.
[23] S.Y. Essack, The development of β-lactam antibiotics in response to the evolution of β-lactamases, Pharm. Res. 18 (10) (2001) 1391–1399.
[24] F.M. Özsoy, O. Öncül, A. Yıldırım, A. Pahsa, Extended-spectrum beta-lactamases: the clinical significance and bring its the problems, Flora 6 (2001) 3–21.
[25] C.C. Sanders, β-lactamases of gram-negative bacteria: new challenges for new drugs, Clin. Infect. Dis. 14 (5) (1992) 1089–1099.
[26] M.J. Frisch, G.W. Trucks, H.B. Schlegel, G.E. Scuseria, M.A. Robb, J.R. Cheeseman, G. Scalmani, V. Barone, B. Mennucci, G.A. Petersson, et al., R.A. Gaussian09, 1, Gaussian, Inc., Wallingford ct, 2009.
[27] R. Dennington, T. Keith, J. Millam, GaussView, version 5, Semichem Inc., Shawnee Mission, KS, 2009.
[28] R. Ditchfield, W.J. Hehre, J.A. Pople, Self-consistent molecular-orbital methods. IX. An extended Gaussian-type basis for molecular-orbital studies of organic molecules, J. Chem. Phys. 54 (2) (1971) 724–728.
[29] A.D. Becke, Density-functional exchange-energy approximation with correct asymptotic behavior, Phys. Rev. A 38 (6) (1988) 3098.
[30] A.D. Becke, A new mixing of Hartree–Fock and local density-functional theories, J. Chem. Phys. 98 (2) (1993) 1372–1377.
[31] A.D. Becke, Density-functional thermochemistry. III. The role of exact exchange, J. Chem. Phys. 98 (7) (1993) 5648–5652.
[32] C. Lee, W. Yang, R.G. Parr, Development of the Colle-Salvetti correlation-energy formula into a functional of the electron density, Phys. Rev. B 37 (2) (1988) 785.
[33] P.J. Hay, W.R. Wadt, Ab initio effective core potentials for molecular calculations. Potentials for the transition metal atoms Sc to Hg, J. Chem. Phys. 82 (1) (1985) 270–283.
[34] W.R. Wadt, P.J. Hay, Ab initio effective core potentials for molecular calculations. Potentials for main group elements Na to Bi, J. Chem. Phys. 82 (1) (1985) 284–298.
[35] P.J. Hay, W.R. Wadt, Ab initio effective core potentials for molecular calculations. Potentials for K to Au including the outermost core orbitals, J. Chem. Phys. 82 (1) (1985) 299–310.
[36] M. Jamróz, J.C. Dobrowolski, Potential energy distribution (PED) analysis of DFT calculated IR spectra of the most stable Li, Na, and Cu (I) diformate molecules, J. Mol. Struct. 565 (2001) 475–480.
[37] O. Trott, A.J. Olson, AutoDock Vina: improving the speed and accuracy of docking with a new scoring function, efficient optimization, and multithreading, J. Comput. Chem. 31 (2) (2010) 455–461.
[38] Dassault Systèmes BIOVIA, Discovery Studio Modeling Environment, Release 4.5, Dassault Systemes, San Diego, 2015.
[39] A.C. Cope, F. Kagan, Cyclic polyolefins. XLII. 3, 3, 7, 7-Tetracarbethoxybicyclo [3.3. 0] oct-1(5)-ene and 3, 3, 7, 7-Tetracarbethoxycycloöctane-1, 5-dione, J. Am. Chem. Soc. 80 (20) (1958) 5499–5502.
[40] A. Bruker, APEX2, V2008. 6, SADABS V2008/1, SAINT V7. 60A, SHELXTL V6. 14, Bruker AXS Inc, Madison, Wisconsin, USA, 2008.
[41] G.M. Sheldrick, SHELXT–Integrated space-group and crystal-structure determination, Acta Crystallogr. Sect. A Found. Adv. 71 (2015) 3–8.
[42] G.M. Sheldrick, Crystal structure refinement with SHELXL, Acta Crystallogr. Sect. C. Struct. Chem. 71 (1) (2015) 3–8.
[43] L.J. Farrugia, ORTEP-3 for windows-a version of ORTEP-III with a graphical user interface (GUI), J. Appl. Crystallogr. 30 (5) (1997), 565–565.
[44] L.J. Farrugia, WinGX suite for small-molecule single-crystal crystallography, J. Appl. Crystallogr. 32 (4) (1999) 837–838.
[45] C.F. Macrae, I.J. Bruno, J.A. Chisholm, P.R. Edgington, P. McCabe, E. Pidcock, L. Rodriguez-Monge, R. Taylor, J.v. Streek, P.A. Wood, Mercury CSD 2.0–new features for the visualization and investigation of crystal structures, J. Appl. Crystallogr. 41 (2) (2008) 466–470.
[46] M. Er, R. Ustabaş, U. Çoruh, K. Sancak, E. Vázquez-López, Synthesis and characterization of some new tetraaldehyde and tetraketone derivatives and X-ray Structure of 1, 1′-(4, 4′-(2-(1, 3-bis (4-Acetylphenoxy) propan-2-ylidene) propane-1, 3-diyl) bis (oxy) bis (4, 1-phenylene)) diethanone, Int. J. Mol. Sci. 9 (6) (2008) 1000–1007.
[47] R. Ustabaş, U. Çoruh, M. Er, K. Serbest, E.M. Vazquez-Lopez, 2, 2′-[2, 3-Bis (1-formyl-2-naphthyloxymethyl) but-2-ene-1, 4-diyldioxy] bis (naphthalene-1-carbaldehyde), Acta Crystallogr. Sect. Sect. E Struct. Rep. Online 62 (11) (2006) o5006–o5007.
[48] J. Wang, W. Wang, H.-J. Chi, Q.-S. Yang, Trans-2, 2′-[(2-Butene-1, 4-diyl) dithio] bis (4, 5-dihydro-1, 3-thiazine), Acta Crystallogr. Sect. Sect. E Struct. Rep. Online 62 (10) (2006) o4621–o4622.
[49] Y. Köysal, S. Öztürk Yildirim, R.J. Butcher, E. Düğdü, 1, 1, 2, 2–Tetrakis [2, 4-dichloro-6-(diethoxymethyl) phenoxymethyl] ethene, Acta Crystallogr. Sect. Sect. E Struct. Rep. Online 68 (10) (2012) o2993–o2994.
[50] National institute of standards and technology (NIST). Computational chemistry comparison and benchmark database Available from: <http://cccbdb.nist.gov/vibscalejust.asp>. Access 15.06.11.
[51] M. Er, Y. Ünver, K. Sancak, E. Dügdü, Synthesis and characterizations of some new tetra-thiosemicarbazones and their cyclization reactions; tetra-4-methyl-5-etoxycarbonyl-2, 3-dihydro-1, 3-thiazole and tetra-2-acetylamino-4-acetyl-4, 5-dihydro-1, 3, 4-thiodiazole derivatives, Arkivoc 15 (2008) 99–120.
[52] M. Er, Y. Ünver, K. Sancak, İ. Değirmencioğlu, Ş.A. Karaogluc, Synthesis, characterization and cyclization reactions of some new bisthiosemicarbazones, Arkivoc 2 (2009) 149–167.
[53] N.P. Roeges, A Guide to the Complete Interpretation of Infrared Spectra of Organic Structures, Wiley, 1994.
[54] R.G. Parr, W. Yang, Density Functional Theory of Atoms and Molecules, Oxford University Press, Oxford, New York, 1989.
[55] R.K. Singh, A.K. Singh, Synthesis, molecular structure, spectral analysis, natural bond order and intramolecular interactions of 2-acetylpyridine thiosemicarbazone: a combined DFT and AIM approach, J. Mol. Struct. 1094 (2015) 61–72.
[56] R. Ditchfield, Molecular orbital theory of magnetic shielding and magnetic susceptibility, J. Chem. Phys. 56 (11) (1972) 5688–5691.
[57] K. Wolinski, J.F. Hinton, P. Pulay, Efficient implementation of the gauge-independent atomic orbital method for NMR chemical shift calculations, J. Am. Chem. Soc. 112 (23) (1990) 8251–8260.
[58] G. Aguirre, L. Boiani, H. Cerecetto, M. Fernández, M. González, A. Denicola, L. Otero, D. Gambino, C. Rigol, C. Olea-Azar, In vitro activity and mechanism of action against the protozoan parasite Trypanosoma cruzi of 5-nitrofuryl containing thiosemicarbazones, Biorg. Med. Chem. 12 (18) (2004) 4885–4893.
[59] C. Soykan, İ. Erol, Synthesis, characterization, and biological activity of N-(4-acetylphenyl) maleimide and its oxime, carbazone, thiosemicarbazone derivatives and their polymers, J. Polym. Sci. Part A Polym. Chem. 41 (13) (2003) 1942–1951.
[60] M. Joseph, V. Suni, C.R. Nayar, M. Kurup, Hoong-Kun Fun, Synthesis, spectral characterization and crystal structure of 2-benzylpyridine N (4) cyclohexylthiosemicarbazone, J. Mol. Struct. 705 (2004) 63–70.
[61] G. Chauvière, B. Bouteille, B. Enanga, C. de Albuquerque, S.L. Croft, M. Dumas, J. Périé, Synthesis and biological activity of Nitro Heterocycles Analogous to Megazol, a trypanocidal Lead, J. Med. Chem. 46 (3) (2003) 427–440.
[62] L. Adrio, G. Alberdi, A. Amoede, D. Lata, A. Fernandez, J. Martinez, M.T. Pereira, J.M.Z. Vila, Synthesis and characterization of pyrrolthiosemicarbazone complexes of palladium(II). Crystal structures of [{Pd[$C_4H_4NC(H)$=NNC(S)NHMe](Cl)}$_2${μ-$Ph_2P(CH_2)_3PPh_2$}] and [Pd{$C_4H_4NC(H)$=NNC(S)NHMe}{$Ph_2P(CH_2)_2PPh_2$-*P, P*}](Cl), Anorg. Allg. Chem. 631 (2005) 2197–2203.
[63] P.W. Atkins, Physical Chemistry, Oxford University Press, Oxford, 2001.
[64] K. Fukui, Role of frontier orbitals in chemical reactions, Science 218 (1982) 747–754.
[65] A.-N.M. Alaghaz, M.E. Zayed, S.A. Alharbi, R.A. Ammar, A. Elhenawy, Synthesis, characterization, biological activity, molecular modeling and docking studies of complexes 4-(4-hydroxy)-3-(2-pyrazine-2-carbonyl) hydrazonomethylphenyl-diazen-yl-benzenesulfonamide with manganese (II), cobalt (II), nickel (II), zinc (II) and cadmium (II), J. Mol. Struct. 1084 (2015) 352–367.
[66] R.G. Parr, R.G. Pearson, Absolute hardness: companion parameter to absolute electronegativity, J. Am. Chem. Soc. 105 (26) (1983) 7512–7516.
[67] A.K. Chandra, T. Uchimaru, Hardness profile: a critical study, J. Phys. Chem. A 105 (14) (2001) 3578–3582.
[68] K. Mandal, T. Kar, P. Nandi, S. Bhattacharyya, Theoretical study of the nonlinear polarizabilities in H 2 N and NO 2 substituted chromophores containing two hetero aromatic rings, Chem. Phys. Lett. 376 (1) (2003) 116–124.
[69] P. Nandi, K. Mandal, T. Kar, Effect of structural changes in sesquifulvalene on the intramolecular charge transfer and nonlinear polarizations–a theoretical study, Chem. Phys. Lett. 381 (1) (2003) 230–238.
[70] P.K. Nandi, K. Mandal, T. Kar, Theoretical study of static second-order nonlinear optical properties of push–pull heteroquinonoid dimers, J. Mol. Struct. Theochem 760 (1) (2006) 235–244.
[71] B. Kramer, M. Rarey, T. Lengauer, Evaluation of the FLEXX incremental construction algorithm for protein–ligand docking, Proteins: Structure, Function, and Bioinformatics 37 (2) (1999) 228–241.